Crystal field and magnetic structure of UO_2

Fei Zhou (周非) and Vidvuds Ozoliņš
Department of Materials Science and Engineering, University of California, Los Angeles, California 90095, USA
(Received 6 January 2011; published 23 February 2011)

The properties of UO_2 result from rich f-electron physics, including electronic Coulomb interactions, spin-orbit and crystal-field effects, as well as interionic multipolar coupling. We present a comprehensive theoretical study of the electronic structure of UO_2 using a combined application of self-consistent DFT + U calculations and a model Hamiltonian. The Γ_5 ground state of U^{4+} and the energies of crystal-field excitations $\Gamma_5 \rightarrow \Gamma_{3,4,1}$ are reproduced in very good agreement with experiment. We also investigate competing noncollinear magnetic structures and confirm 3k as the $T = 0$ K ground-state magnetic structure of UO_2.

DOI: 10.1103/PhysRevB.83.085106 PACS number(s): 71.27.+a, 71.15.Mb, 71.70.Ch

I. INTRODUCTION

Uranium dioxide is an important and interesting material from both technological and scientific perspectives. During the past half-century, the electronic structure of UO_2 has been thoroughly characterized by various experiments[1–12] (for a recent review, see Ref. 13). UO_2 is a semiconductor with a 2-eV band gap[1] and localized $5f^2$ electrons that retain strong atomiclike properties. Due to significant Coulomb interactions and spin-orbit (SO) effects, the ground state of a free U^{4+} ion is the $^3H_4$ nonet [see Fig. 1(a)]. When the crystal field (CF) of UO_2's fluorite structure is considered, $^3H_4$ is split into the ground-state Γ_5 triplet and the excited Γ_3 doublet, Γ_4 triplet, and Γ_1 singlet, all approximately 0.15 eV above Γ_5[6,9] [see Fig. 1(b)]. When cooled below $T_N = 30.8$ K, UO_2 undergoes a first-order phase transition from a paramagnetic to a transverse type-I antiferromagnetic (AF) phase,[2] which exhibits a Jahn-Teller (JT) distortion of the oxygen cage.[5] Experimental studies now converge on the view that the noncollinear magnetic structure and the oxygen distortion are of the 3k type;[7,9–11] that is, the moment and lattice distortion are both along the $\langle 111 \rangle$ direction [see Fig. 1(c)], instead of the previously proposed 1k ($\langle 001 \rangle$)[14] and 2k ($\langle 110 \rangle$)[5] structures.

On the theory side, the CF model of Rahman and Runciman[15] correctly predicted the Γ_5 ground state of UO_2 (Fig. 2). Recent CF calculations have obtained quantitative agreement with experimental excitation spectra by fitting model parameters to the measured data,[16] by adding corrections to the point charge model,[17] or by extrapolating from the fitted values for other actinide dioxides.[18] Models of magnetism in UO_2, pioneered by the work of Allen,[14] have explored the delicate interplay between multipolar and JT effects.[13]

First-principles calculations have to go beyond the local-density or generalized-gradient approximations (LDA/GGA) to the density functional theory (DFT) to correctly reproduce the insulating character of UO_2. Existence of an energy gap was demonstrated in Refs. 19 and 20 using the hybrid functional method,[21] in Ref. 22 using the self-interaction-corrected LDA,[23] and in Ref. 24 using the DFT + U method.[25] CF splitting in actinide compounds has been computed by using constrained f states without full self-consistency[26] or by analyzing band positions obtained from LDA/GGA calculations.[27] The 3k structure of UO_2 was studied by Laskowski *et al.* using DFT + U,[28] but their results showed anomalous dependence on the U parameter and both the calculated oxygen distortions and energy differences were about an order of magnitude too large. Furthermore, the 3k state was only stable with large U values and a formulation of DFT + U that is usually only applied to metals. A first-principles framework for self-consistently and accurately accounting for all the different energy scales in Fig. 1 does not yet exist.

In this paper, we present a unified DFT-based framework for calculating the electronic spectra, magnetism, and lattice distortions in UO_2. Explicit f-f interactions and CF effects are treated using a model Hamiltonian with parameters derived from self-consistent DFT + U calculations. The ground-state wave functions that are obtained by diagonalizing this Hamiltonian are used to set up initial conditions for self-consistent DFT + U calculations of magnetism and lattice relaxations. Our approach allows us to accurately reproduce all the different energy scales in Fig. 1, including the Γ_5 ground state, $\Gamma_{3,4,1}$ excited states, as well as the energetics of competing magnetic structures, including 3k, and their associated lattice distortions, all within a unified self-consistent framework.

Before moving on to the details, we stress that extra care should be taken in first-principles calculations of f electrons. Several challenges are encountered in DFT calculations of UO_2 (and other actinide compounds in general). First, strong f-f interactions and a weak CF result in an inherently complicated many-body problem. For instance, since $5f^2$ electrons hybridize weakly with the O $2p$ bands and remain well localized, their true wave functions are in general multideterminantal (see below for further discussions). Second, the higly localized nature of f electrons tends to magnify the inaccuracies of approximate exchange-correlation functionals. We have previously shown that the self-interaction (SI) error of f electrons is highly sensitive to the occupied orbital, and its removal is nontrivial in both the DFT + U and hybrid-functional methods.[29] Therefore, an improved version of DFT + U[29] is required to remove such errors (∼0.1 eV) and access weak CF effects. Third, the existence of a multitude of f states often leaves DFT + U calculations trapped in local minima, leading to difficulties in reproducibly finding the correct electronic ground state. As a consequence, it is not uncommon for different authors to find inconsistent and

1098-0121/2011/83(8)/085106(6)

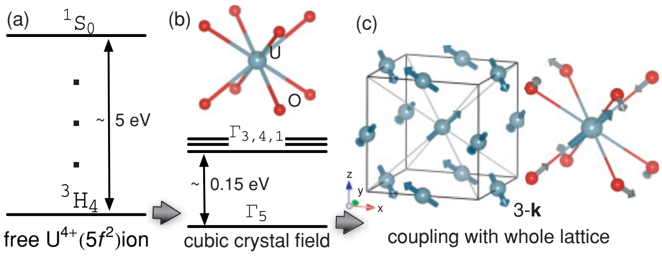

FIG. 1. (Color online) Schematics of the $5f^2$ ground states and level splitting, in decreasing interaction strength, of (a) free U^{4+} ion, (b) cubic CF, and (c) ordered 3k noncollinear magnetic structure of bulk UO_2: left, direction of magnetic moments on uranium, designated by large arrows; right, distortion of oxygen (small arrows) around a central U atom.

hard-to-interpret results with large errors (~1 eV or even larger) even when using identical electronic-structure methods (see Refs. 29–36 and references therein). It is likely that this issue contributed to the failure of previous studies to reliably examine the 3k structure of UO_2.[28] Previously, we have shown that the local minima issue is also present in hybrid functional calculations.[29] In this paper, we show that the multiple minima, corresponding to different orbital states, contain valuable physical information about f electrons that can be used to help find the true ground state and excitation spectra.

II. METHOD

A. LDA + U calculations

All DFT calculations were carried out using the VASP code,[37] GGA-PAW potentials,[38] a cutoff energy of 450 eV, and without any symmetry constraints to allow symmetry-breaking solutions. Crystal-field calculations were performed in the primitive cell of one UO_2 formula unit with a $6 \times 6 \times 6$ k-point grid. The lattice and ionic positions were frozen at the experimental fluorite structure for CF calculations. These calculations, as discussed in Sec. III A, are ferromagnetic with one uranium ion per cell. Magnetic structures were calculated in the fcc supercell (four formula units) using a $4 \times 4 \times 4$ grid, first without and then with full relaxation. Spin-orbit coupling was self-consistently incorporated for realistic comparison with experiment.

To remove the orbital-dependent components of SI errors (SIEs) of f electrons, we use a formulation of the LDA + U method[29] by modifying only the exchange term, rather than both Hartree and exchange, of the LDA:

$$E^{\mathrm{LDA}+U} = E^{\mathrm{LDA}} + E_{\mathrm{X}} - E_{\mathrm{dcX}}, \tag{1}$$

where the orbital-dependent Hartree-Fock exchange E_{X} contains a term that approximately cancels the on-site SIE in the Hartree energy of localized f electrons; the remainder of the LDA Hartree energy is exact by definition and therefore left unmodified in our approach. The exchange double-counting term E_{dcX} accounts for the LDA exchange energy and is given by a linear combination controlled by the c parameter of the exchange double-counting in the Liechtenstein[39] scheme and the on-site local-spin-density (LSD) exchange, conceptually similar to hybrid functional approaches and serves the purpose of subtracting the orbital-dependence of the LDA exchange energy. As a result, Eq. (1) is SI free to high accuracy.

There is only one adjustable parameter, U, in our approach, and the other parameters J and c can be determined at given U. As done in Ref. 29, we choose up to seven f^2 SSD states of the U^{4+} ion that are analytically degenerate without considering SO and calculate these states' total energy dependence on J and c. As shown in Fig. 3, optimal values of $J = 0.6$ eV and $c = 0.5$ are obtained at $U = 6$ eV that minimize the energy difference, that is, the orbital-dependent SIE. These J and c values are used throughout the paper. We use $U = 6$ eV in this paper and discuss the dependence of

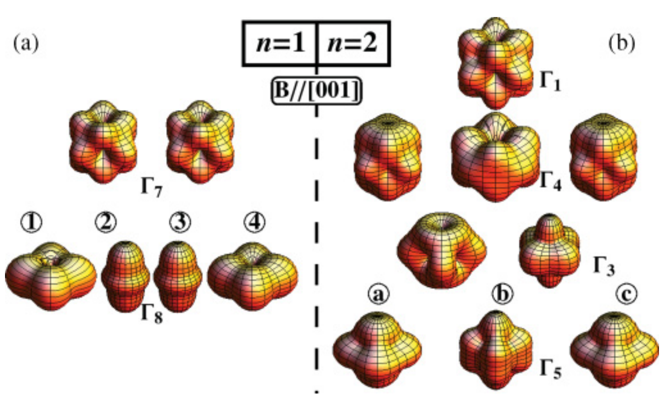

FIG. 2. (Color online) Low-energy f^n eigenstates of Hamiltonian (2). (a) $n = 1$, Γ_8 ground states and Γ_7 doublet of the $j = 5/2$ sextet; (b) $n = 2$, Γ_5 ground states and the excited $\Gamma_{3,4,1}$ of $^3H_4$.

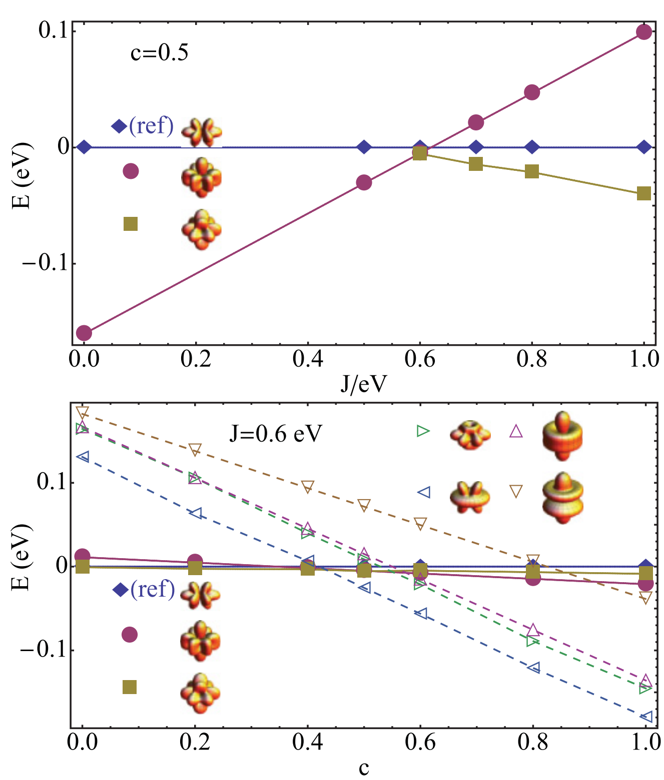

FIG. 3. (Color online) LDA + U energy of U^{4+} ion as function of J in different orbitals. SOC is not included.

TABLE I. For different magnetization directions $\boldsymbol{B}$, the ground states Γ_8 quartet (f^1) and Γ_5 triplet (f^2), their spin and total magnetic moment in μ_B, and, for f^2, the dominant determinants in the corresponding f^1 basis.

	$n = 1$			$n = 2$			
B	Γ_8	μ_S	μ	Γ_5	State	μ_S	μ
[001]	1 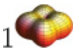	−0.54	1.57	a 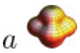	0.97(1,2)	−0.86	2.06
	2 	−0.13	0.43	b 	0.69[(1,3)	0.00	0.00
	3 	0.13	−0.43		+(2,4)]		
	4 	0.54	−1.57	c 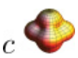	0.97(3,4)	0.86	−2.06
[110]	1 	−0.48	1.40	a 	0.92(1,2)	−0.86	2.06
	2 	−0.28	0.83	b 	0.69[(1,3)	0.00	0.00
	3 	0.28	−0.83		+(2,4)]		
	4 	0.48	−1.40	c 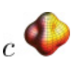	0.92(3,4)	0.86	−2.06
[111]	1 	−0.44	1.28	a 	0.92(1,2)	−0.86	2.06
	2 	−0.33	1.00	b 	0.69[(1,4)	0.00	0.00
	3 	0.33	−1.00		+(2,3)]		
	4 	0.44	−1.28	c 	0.92(3,4)	0.86	−2.06

the results on U in Sec. III B. In the rest of the paper SO is included.

B. On-site model Hamiltonian for f

We consider the following single-ion model for f electrons:

$$H_0 = \sum_{i=1}^{n} (\hat{f}_i + \zeta \hat{\boldsymbol{l}}_i \cdot \hat{\boldsymbol{s}}_i) + \hat{V}_{ee}, \quad (2)$$

where the summation runs over n electrons for the one-body terms of cubic CF, $\hat{f}$, and SO coupling of strength ζ. The electronic interaction $\hat{V}_{ee}$ is parametrized by Slater's integrals F^k ($k = 0,2,4,6$).[40] The matrix elements of $\hat{f}$ between the basis states indexed by projections of orbital (m) and spin (σ) momenta are given by

$$\langle m\sigma|\hat{f}|m'\sigma'\rangle = \delta_{\sigma\sigma'} \int \bar{Y}^l_m \left[\frac{16\sqrt{\pi}}{3} V_4 \left(Y_{40} + \sqrt{\frac{10}{7}} \mathrm{Re} Y_{44} \right) + 32\sqrt{\frac{\pi}{13}} V_6 (Y_{60} - \sqrt{14} \mathrm{Re} Y_{64}) \right] Y^l_{m'} d\Omega, \quad (3)$$

where $V_{4,6}$ are cubic CF parameters[41] and Y^l_m are complex spherical harmonics. To study the magnetic properties, an infinitesimal magnetization field $\boldsymbol{B}$ (B $\to$ 0) is applied:

$$H' = H_0 - \sum_{i=1}^{n} \boldsymbol{B} \cdot (g_L \hat{\boldsymbol{l}}_i + g_S \hat{\boldsymbol{s}}_i) \mu_B / \hbar, \quad (4)$$

where $g_L = 1$ and $g_S \approx 2$ are the orbital and spin g factors, respectively.

We first discuss the general properties of solutions to Eqs. (2)–(4) using the model parameters derived from DFT + U calculations (which are discussed in detail in Sec. III A). For $n = 1$, 14 eigenstates are obtained, the lowest being the Γ_8 quartet (Fig. 2 and Table I). For $n > 1$, the Hamiltonian in Eq. (2) can be diagonalized via configuration interaction of C^{14}_n f^n single Slater determinants (SSDs) based on the f^1 eigenstates. The Γ_5 ground states of f^2 are shown in Table I, together with their dominant determinants, designated as (i,j) using the indices of f^1 states in the left column of Table I. For magnetic moment along each of the [001], [110], and [111] directions, the Γ_8 quartet of f^1 includes states 1,4 (2,3) with larger (smaller) spin and orbital magnetic momenta, while the Γ_5 triplet of f^2 consists of states a and c with $|\mu| = 2.06$ μ_B and one dominant determinant [(1,2) or (3,4)], as well as a nonmagnetic state b dominated by two determinants (right column of Table I). Note that the observed moment of the ordered state is smaller at 1.75 μ_B.[5] The moment $\mu = 2.06\mu_B$ of the $\Gamma_5(a,c)$ states is slightly larger than the saturated $2\mu_B$ characteristic of the $^3H_4$ multiplet because exchange and SOC interactions are all of comparable strength and other multiplets slightly mix into the ground state and increase the effective moment.[15] In general, all the f^2 eigenstates, including $\Gamma_{3,4,1}$ (Fig. 2) are composed of multiple determinants.

C. Model parameters from LDA + U

The parameters for the model Hamiltonian in Eq. (2) are obtained by analyzing the total energies and f wave functions calculated with LDA + U. In this procedure, many self-consistent LDA + U calculations are first carried out, yielding solutions that are in general local minima rather than the global minimum of UO_2. Next, we extract the f^2 Kohn-Sham wave function $|\Psi_f\rangle$, SSD by construction, from each solution, and compute the expected energy according to Eq. (2),

$$\langle\Psi_f|H_0|\Psi_f\rangle = x_1V_4 + x_2V_6 + x_3\zeta + x_4F^2 + U, \quad (5)$$

where x_i's represent the solution-dependent coefficient associated with model parameters. Since the F^k ($k = 2,4,6$) contributions of $\hat{V}_{ee}$ are heavily correlated,[42] the following approximation[43] has been adopted in Eq. (5),

$$F^2 = F^4/0.668 = F^6/0.494, \quad (6)$$

eliminating model parameters F^4 and F^6. Finally, expectation values of H [Eq. (5)] of the obtained solutions are fitted to the corresponding DFT + U total energies, yielding self-consistent *ab initio* values of F^2, ζ, and the CF parameters V_4 and V_6. We use the simple least-squares method to perform the linear fitting. Here U in Eq. (5) can be regarded as a constant in the fitting and bears no direct physical meaning.

III. RESULTS AND DISCUSSIONS

A. Crystal-field ground states and excitations

We carried out a series of 50 different self-consistent calculations with randomly initialized f^2 states. Due to the existence of multiple local minima in DFT + U, these calculations resulted in a range of energies spread over almost 2 eV [solid circles in Fig. 4(a)]. It is seen that random wave function initialization has generated only one low-energy solution, while the remaining runs were trapped in metastable high-energy states.

Obtained from the fitting procedure outlined in Sec. II C, model parameters are applied in Eq. (2) to construct f^1 eigenstates and subsequently determine f^2 states by direct diagonalization within the subspace of SSDs formed from f^1 eigenstates. To further improve the quality of our fit and provide data points in the low-energy region that was poorly represented in the randomly initialized sample [solid circles in Fig. 4(a)], we self-consistently calculate the DFT + U energies of additional 15 two-electron SSD states that involve the

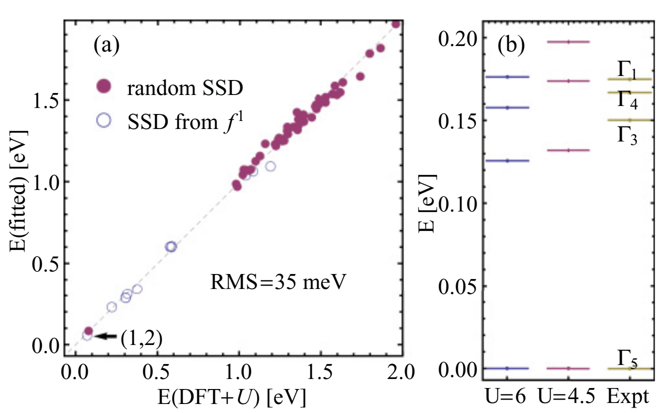

FIG. 4. (Color online) (a) Fitting of DFT + U (Ref. 29) energy to Eq. (2) for 50 runs with random initial states (solid circles) and 15 states with initial states constructed from f^1 solutions (open circles). (b) Predicted f^2 CF levels $\Gamma_{5,3,4,1}$ compared to measured CF splitting (Ref. 9).

TABLE II. Fitted parameters (in eV) using Eqs. (2), (3), and (6), compared with prior studies.

	F^2	F^4	F^6	ζ	V_4	V_6
$U = 6$ eV	5.649	(3.773)	(2.790)	0.230	−0.093	0.0157
$U = 4.5$ eV	5.495	(3.670)	(2.714)	0.209	−0.106	0.0163
U^{4+} ion (Ref. 44)	6.439	5.295	3.440	0.244		
Ref. 16		Using Ref. 44			−0.112	0.024
Ref. 9					−0.123	0.0265
Ref. 18					−0.155	0.0333

6 low-energy f^1 orbitals (Γ_8 and Γ_7) for $\boldsymbol{B}//[001]$; these points are shown as open circles in Fig. 4(a). The (1,2) and (3,4) states, which dominate the Γ_{5a} and Γ_{5c} ground states, are also found to have the lowest energies in self-consistent DFT + U calculations, demonstrating that our method can reliably locate the electronic ground state. The other ground state in Table I, Γ_{5b}, has two dominant determinants and is not directly accessible in DFT + U. Therefore, the data flow between the model Hamiltonian and DFT + U calculations is bidirectional: DFT + U provides model parameters, while the model guides the DFT + U to the ground state and gives access to multideterminant states.

The final fitted parameters are shown in Table II. Compared to the values obtained by fitting the spectra of free ions,[44] the ionic parameters F^k, and ζ in the UO_2 solid are somewhat suppressed due to hybridization and screening effects. The calculated cubic CF parameters V_4 and V_6 are slightly smaller than those fitted to experimental data or extrapolated from other actinide oxides.[9,16,18] The Hamiltonian in Eq. (2) can now be diagonalized. The predicted energies of the three lowest excited CF levels $\Gamma_{3,4,1}$ are in reasonable agreement with experiment[9] with errors of approximately 10–20 meV [Fig. 4(b)]. A notable deviation is overestimation of the splitting between these levels.

Finally, we note that the input $J = 0.6$ eV used in our DFT + U calculation differs from the fitted value of $J' = (286F^2 + 195F^4 + 250F^6)/6435$ in Table II. This is because the role of the former is to minimize the SIE in DFT + U, while the latter represents on-site exchange, and some difference between them is expected when used with an approximate XC functional. A perfect XC functional would make the input U or J unnecessary and predict physically meaningful output J' or F^k.

B. Dependence on input U

To illustrate the effect of the only adjustable variable in our approach, U, the same calculations were repeated using $U = 4.5$ eV. As shown in Table II and Fig. 4(b), the results change only slightly and remain in good agreement with experiment. Note that when U, which controls the degree of electron localization, is decreased, the ionic parameters F^k and ζ also decrease, that is, away from the free ion values, while the CF parameters increase, suggesting that the f electrons become more delocalized. Such a picture of opposite influence of electron localization on free ion and CF parameters is consistent with the observed trend that increase of the CF

TABLE III. Energy (in meV per UO_2) for different magnetic structures, without and with ionic relaxation.

	Static			Relaxed		
Configuration	E_s	$E_s - E_d$	$\lvert\mu\rvert/\mu_B$	E_r	$E_r - E_d$	$\lvert\mu\rvert/\mu_B$
[001] FM	0 (ref)	3.3	2.11	−57.3	−54.0	2.20
[001] AAF	−6.5	−3.3	2.11	−61.9	−58.6	2.35
[110] FM	−8.2	2.1	2.15	−65.5	−55.2	2.33
[110] AAF	−12.4	−2.1	2.15	−71.8	−61.5	2.22
[111] FM	−8.5	2.4	2.22	−70.3	−59.5	2.22
[111] AAF	−13.2	−2.4	2.21	−76.3	−65.5	2.27
3k	−13.8	−3.0	2.21	−81.1	**−70.3**	2.39

interaction results in a reduction in the free-ion parameters for the same ion in different chemical environment.[45]

C. Magnetic properties

Finally, we discuss the effects of interionic interactions and magnetic properties of UO_2. Various magnetic structures within a cubic supercell of four formula units were calculated, first without and then with lattice relaxation. The previous approximation of representing the Γ_5 ground state with the (1,2),(3,4) SSDs was adopted. Table III shows the energies E_s (static lattice), E_r (after full relaxation), and the total magnetic moments μ assuming ferromagnetic (FM) and type-A antiferromagnetic (AAF) configurations along the [001] (reference), [110], and [111] directions. In all cases, the calculated μ of ∼2.1–2.2 μ_B is close to the saturated value 2.06 μ_B in Table I and larger than the measured 1.74 μ_B[2]. The reduction of the ordered moment is a topic of considerable interest, but the mechanisms, such as the dynamical JT effect,[46] are beyond the scope of this work. Given that the (1,2)/(3,4) states are the CF ground states within our computational approach and the calculated moment is not too far from 1.74 μ_B, we continue to use these settings for noncollinear magnetic calculations.

Table III shows that for each magnetization direction, the AAF configuration is always lower than the FM configuration, in agreement with experiment. The energy differences $E_s(\mathrm{FM}) - E_s(\mathrm{AAF})$ are in the 4-to-6-meV range, suggesting that multipolar interactions and anisotropy are weak. These weak, mostly isotropic interactions underlie the success of the simple fitting procedure of Sec. II C (root-mean-square error = 35 meV) in FM configurations of 15 ⟨001⟩ solutions and 50 solutions with random magnetic moment directions. We also find that the different magnetization directions differ in energy by less than 9 meV, suggesting that our procedure for removing the orbital-depedent SIE is highly accurate. Indeed, the f^2 wave functions differ considerably for the three principle directions (see Table I), which would result in SIEs of 0.1–0.2 eV using the unmodified DFT + U approach. Nevertheless, we take additional care to remove any remaining SIEs, however small they they appear to be, by subtracting a reference energy E_d for each principle magnetization direction $d = \langle 001\rangle$, $\langle 110\rangle$, or $\langle 111\rangle$: $E_d = [E_s(\mathrm{FM}) + E_s(\mathrm{AAF})]/2$. With this correction, the AAF configurations in the three directions, as well as the 3k structure [magnetic moment along ⟨111⟩, see Fig. 1(c)], are essentially degenerate before lattice relaxation.

The magnetic transition temperature of UO_2 is estimated with a classical Heisenberg model on an fcc lattice:

$$\mathcal{H} = -J_H \sum_{\langle ij\rangle} \vec{s}_i \cdot \vec{s}_j, \tag{7}$$

where the summation is over all nearest-neighbor sites $\langle ij\rangle$ with unit spin $\vec{s}$. The FM/AAF energy difference per UO_2 is $\Delta E = 6J_H - (-2J_H) = 8J_H$. As shown in Table III, $\Delta E \approx$ 6 meV, corresponding to $T_N = 3.18 J_H/k_B$,[47] or about 28 K, in excellent agreement with the experimental value 30.8 K.[2]

After relaxation without symmetry constraints, we obtain the energies listed in the right column of Table III. The computed moments μ become slightly larger than the static values. The relaxation energy E_r and the corrected $E_r - E_d$ are large (>50 meV) due to differences between the static (fixed to experimental $a = 5.47$ Å) and relaxed lattice parameters. The energy differences between competing magnetic configurations increases to ∼10 meV; these values are consistent with the Néel temperature of $T_N = 30.8$ K .[2] The relaxed structures with $\mu//\langle 111\rangle$ are clearly more stable than ⟨001⟩ and ⟨110⟩. We have enumerated all AF ⟨111⟩ structures within the fcc unit cell and found that the 3k structure indeed has the lowest energy. The associated oxygen lattice distortion (amplitude 0.024 Å) is also of the 3k type, though slightly larger than the measured 0.014 Å.[5]

IV. CONCLUSIONS

In summary, we have studied the electronic structure of UO_2 using an aspherical-SI free DFT + U method coupled with a model Hamiltonian. The Γ_5 CF ground states, as well as the CF excitation energies are reproduced in good agreement with experiment. Various magnetic structures are investigated with careful initialization of the orbital and magnetic states. The interionic interactions are found to be weak and largely isotropic. When SIEs are accounted for, the 3k structure is essentially degenerate with other antiferromagnetic configurations and becomes the ground state only when lattice relaxations are considered. Our work demonstrates the usefulness of electronic structure calculations for f compounds with proper treatment of SIEs and multiple self-consistent local minima corresponding to different orbital states; this approach can be readily applied to defect supercells and other f compounds.

ACKNOWLEDGMENTS

This work was supported by the US Department of Energy, Nuclear Energy Research Initiative Consortium (NERI-C), under Grant No. DE-FG07-07ID14893 and used resources of the National Energy Research Scientific Computing Center (NERSC).

[1] J. Schoenes, Phys. Rep. **63**, 301 (1980).
[2] B. C. Frazer, G. Shirane, D. E. Cox, and C. E. Olsen, Phys. Rev. **140**, A1448 (1965).
[3] B. T. M. Willis and R. I. Taylor, Phys. Lett. **17**, 188 (1965).
[4] R. A. Cowley and G. Dolling, Phys. Rev. **167**, 464 (1968).
[5] J. Faber, G. H. Lander, and B. R. Cooper, Phys. Rev. Lett. **35**, 1770 (1975).
[6] S. Kern, C. K. Loong, and G. H. Lander, Phys. Rev. B **32**, 3051 (1985).
[7] P. Burlet, J. Rossatmignod, S. Quezel, O. Vogt, J. C. Spirlet, and J. Rebizant, J. Less-Common Met. **121**, 121 (1986).
[8] R. Osborn, A. D. Taylor, Z. A. Bowden, M. A. Hackett, W. Hayes, M. T. Hutchings, G. Amoretti, R. Caciuffo, A. Blaise, and J. M. Fournier, J. Phys. C **21**, L931 (1988).
[9] G. Amoretti, A. Blaise, R. Caciuffo, J. M. Fournier, M. T. Hutchings, R. Osborn, and A. D. Taylor, Phys. Rev. B **40**, 1856 (1989).
[10] K. Ikushima, S. Tsutsui, Y. Haga, H. Yasuoka, R. E. Walstedt, N. M. Masaki, A. Nakamura, S. Nasu, and K. Onuski, Phys. Rev. B **63**, 104404 (2001).
[11] E. Blackburn, R. Caciuffo, N. Magnani, P. Santini, P. J. Brown, M. Enderle, and G. H. Lander, Phys. Rev. B **72**, 184411 (2005).
[12] S. B. Wilkins, R. Caciuffo, C. Detlefs, J. Rebizant, E. Colineau, F. Wastin, and G. H. Lander, Phys. Rev. B **73**, 060406 (2006).
[13] P. Santini, S. Carretta, G. Amoretti, R. Caciuffo, N. Magnani, and G. H. Lander, Rev. Mod. Phys. **81**, 807 (2009).
[14] S. J. Allen, Phys. Rev. **166**, 530 (1968); **167**, 492 (1968).
[15] H. U. Rahman and W. A. Runciman, J. Phys. Chem. Solids **27**, 1833 (1966).
[16] H. U. Rahman, Phys. Lett. A **240**, 306 (1998).
[17] Z. Gajek, M. P. Lahalle, J. C. Krupa, and J. Mulak, J. Less-Common Met. **139**, 351 (1988).
[18] N. Magnani, P. Santini, G. Amoretti, and R. Caciuffo, Phys. Rev. B **71**, 054405 (2005).
[19] K. N. Kudin, G. E. Scuseria, and R. L. Martin, Phys. Rev. Lett. **89**, 266402 (2002).
[20] I. D. Prodan, G. E. Scuseria, and R. L. Martin, Phys. Rev. B **76**, 033101 (2007).
[21] A. D. Becke, J. Chem. Phys. **98**, 1372 (1993).
[22] L. Petit, A. Svane, Z. Szotek, W. M. Temmerman, and G. M. Stocks, Phys. Rev. B **81**, 045108 (2010).
[23] J. P. Perdew and A. Zunger, Phys. Rev. B **23**, 5048 (1981).
[24] S. L. Dudarev, D. N. Manh, and A. P. Sutton, Philos. Mag. B **75**, 613 (1997).
[25] V. I. Anisimov, J. Zaanen, and O. K. Andersen, Phys. Rev. B **44**, 943 (1991).
[26] M. Colarieti-Tosti, O. Eriksson, L. Nordstrom, J. Wills, and M. S. S. Brooks, Phys. Rev. B **65**, 195102 (2002).
[27] P. Novak and M. Divis, Phys. Status Solidi B **244**, 3168 (2007).
[28] R. Laskowski, G. K. H. Madsen, P. Blaha, and K. Schwarz, Phys. Rev. B **69**, 140408 (2004).
[29] F. Zhou and V. Ozolins, Phys. Rev. B **80**, 125127 (2009).
[30] A. B. Shick, W. E. Pickett, and A. I. Liechtenstein, J. Electron Spectrosc. Relat. Phenom. **114-116**, 753 (2001).
[31] P. Larson, W. R. L. Lambrecht, A. Chantis, and M. van Schilfgaarde, Phys. Rev. B **75**, 045114 (2007).
[32] G. Jomard, B. Amadon, F. Bottin, and M. Torrent, Phys. Rev. B **78**, 075125 (2008).
[33] B. Amadon, F. Jollet, and M. Torrent, Phys. Rev. B **77**, 155104 (2008).
[34] E. R. Ylvisaker, W. E. Pickett, and K. Koepernik, Phys. Rev. B **79**, 035103 (2009).
[35] B. Dorado, B. Amadon, M. Freyss, and M. Bertolus, Phys. Rev. B **79**, 235125 (2009).
[36] B. Meredig, A. Thompson, H. A. Hansen, C. Wolverton, and A. van de Walle, Phys. Rev. B **82**, 195128 (2010).
[37] G. Kresse and D. Joubert, Phys. Rev. B **59**, 1758 (1999).
[38] P. E. Blochl, Phys. Rev. B **50**, 17953 (1994).
[39] A. I. Liechtenstein, V. I. Anisimov, and J. Zaanen, Phys. Rev. B **52**, R5467 (1995).
[40] B. R. Judd, *Operator Techniques in Atomic Spectroscopy* (McGraw-Hill, New York, 1963).
[41] D. Newman and B. Ng, *Crystal Field Handbook* (Cambridge University Press, Cambridge, 2000).
[42] W. T. Carnall, J. Chem. Phys. **96**, 8713 (1992).
[43] M. T. Berry, C. Schwieters, and F. S. Richardson, Chem. Phys. **122**, 105 (1988).
[44] C. H. H. Van Deurzen, K. Rajnak, and J. G. Conway, J. Opt. Soc. Am. B **1**, 45 (1984).
[45] G. K. Liu, J. Solid State Chem. **178**, 489 (2005).
[46] D. Ippolito, L. Martinelli, and G. Bevilacqua, Phys. Rev. B **71**, 064419 (2005).
[47] S. McKenzie, C. Domb, and D. L. Hunter, J. Phys. A **15**, 3899 (1982).